EUROPEAN SYNCHROTRON RADIATION FACILITY

INSTALLATION EUROPEENNE DE RAYONNEMENT SYNCHROTRON

ESRF

Experiment Report Form

The double page inside this form is to be filled in by all users or groups of users who have had access to beam time for measurements at the ESRF.

Once completed, the report should be submitted electronically to the User Office via the User Portal:

https://wwws.esrf.fr/misapps/SMISWebClient/protected/welcome.do

Reports supporting requests for additional beam time

Reports can be submitted independently of new proposals – it is necessary simply to indicate the number of the report(s) supporting a new proposal on the proposal form.

The Review Committees reserve the right to reject new proposals from groups who have not reported on the use of beam time allocated previously.

Reports on experiments relating to long term projects

Proposers awarded beam time for a long term project are required to submit an interim report at the end of each year, irrespective of the number of shifts of beam time they have used.

Published papers

All users must give proper credit to ESRF staff members and proper mention to ESRF facilities which were essential for the results described in any ensuing publication. Further, they are obliged to send to the Joint ESRF/ ILL library the complete reference and the abstract of all papers appearing in print, and resulting from the use of the ESRF.

Should you wish to make more general comments on the experiment, please note them on the User Evaluation Form, and send both the Report and the Evaluation Form to the User Office.

Deadlines for submission of Experimental Reports

- 1st March for experiments carried out up until June of the previous year;
- 1st September for experiments carried out up until January of the same year.

Instructions for preparing your Report

- fill in a separate form for each project or series of measurements.
- type your report, in English.
- include the reference number of the proposal to which the report refers.
- make sure that the text, tables and figures fit into the space available.
- if your work is published or is in press, you may prefer to paste in the abstract, and add full reference details. If the abstract is in a language other than English, please include an English translation.

Names and affiliations of applicants (* indicates experimentalists):

*Dr. JESTIN Jacques ; Laboratoire Léon Brillouin, CEA de Saclay ; 91191 Gif sur Yvette

M. BOUTY Adrien ; Laboratoire Léon Brillouin, CEA de Saclay ; 91191 Gif sur Yvette

*M. GENEVAZ Nicolas ; Laboratoire Léon Brillouin, CEA de Saclay ; 91191 Gif sur Yvette

Dr. OBERDISSE Julian ; Laboratoire Charles Coulomb, Pl. E. Bataillon ; 34095 Montpellier

M. BAEZA Guilhem ; Laboratoire Charles Coulomb, Pl. Eugène Bataillon ; 34095 Montpellier

*Dr. GENIX Anne-Caroline ; Laboratoire Charles Coulomb, Pl. Eugène Bataillon ; 34095 Montpellier

*Dr. BANC Amélie ; Laboratoire Charles Coulomb, Pl. Eugène Bataillon ; 34095 Montpellier

Report:

Thanks to the good eletronic contrast between organic polymers and silica, we successfully measured on ID02 the dispersion of fillers in various nanocomposite systems. Rubber nanocomposites and acrylate latex nanocomposites filled with silica nanoparticles were measured.

Two configurations were used:

- λ=10Å , Sample-Detector distance = 2.5m to scan the q range [$3.5.10^{-3}$ to 0.15 Å^{-1}] Å^{-1}.
- The USAXS setup with the Bonse-Hart camera to reach the q_{min} value 10^{-4} Å^{-1} .

The 2D-data recorded were then processed, using the software SAXS-Utilities avalaible on place. The isotropic average of these scattering patterns around the center of scattering allows to reduce the resulting data to a one-dimension output I(q), with $q^2=q_x^2+q_y^2$. For isotropic sample, the 2D-patterns show a circular symmetry. So, isotropic averaging was done on complete circles. Some samples were measured at stretched state. The resulting 2D-patterns show two axis of symmetry along the two main directions of stretching (the PARAllel one and the PERPendicular one). Data averaging was done along these two directions in 20° bissectors. For each strain rate, we obtained thus a pair of spectra : $I_{PARA}(q)$ (resp. $I_{PERP}(q)$) shows the local reorganizations in the parallel (resp. perpendicular) direction of stretching.

As more than 200 samples were measured during this experiment, only few results are reported here.

Within the framework of Ph.D thesis in partnership with Michelin, we have developed an original solvent casting process allowing the formulation of "model" nanocomposites based on colloidal silica (Ludox TM40 Aldrich) and copolymer (SB).

Previous SAXS results on **model nanocomposites based on graftable SBR chains (D3)** have shown that longer polymer chains (140 kg/mol compared to 40 kg/mol) lead to a better dispersion of the silica nanoparticles.

In this experiment, the silica state in ternary suspensions (silica + polymer + solvent: 2-Butanone) has been investigated for different chain lengths (40 and 140 kg/mol), in order to follow the aggregation kinetics. The filler fraction was varied from 0.55 to 5.7%vol with a constant polymer fraction R_p =8%vol in the suspension. SAXS results obtained for 40kg/mol ternary suspensions are presented in Fig. 1.
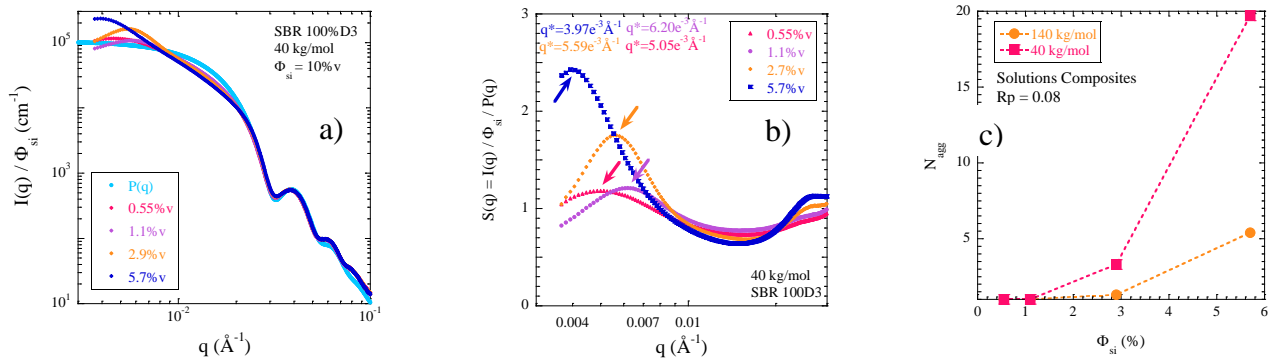

Figure 1: (a) Structural evolution of ternary suspensions as a function of the filler fraction for 40kg/mol SB. (b) is the corresponding structure factors obtained by dividing the scattered intensity by the silica bead form factor. (c) Aggregation number as a function of the filler fraction in ternary suspensions for M = 40 and 140 kg/mol.

Looking at the structure factor (Figs 1 b)), one can clearly see a repulsive peak which evolves with the silica fraction. The peak position characterizes the most probable distance between objects. From 0.55 to 1.1%vol silica, the peak is shifted towards larger angles suggesting a reduction of the inter-bead distance (e.g. adding particles). Then, from 1.1% to 5.7%vol silica, the behavior is opposite with an increase of the inter-bead distance. In this case, the elementary beads form aggregates, and the aggregates centers of mass are separated by larger distances. The same trend is observed for both polymer masses. From a simple cubic model it is possible to evaluate the mean aggregation number in the suspension. These results are presented in Fig.1(c).

Model systems based on non-graftable SBR chains (NF) were studied at rest and under uniaxiale traction.

At rest, dispersion was studied with the type of dispersing agent as the main input: tuned by OCTEO on Fig.1a), tuned by Si69 on Fig.1b). The shoulders pointed by the arrows on Fig.1 show the presence of primary aggregates (aggregation of primary Ludox nanoparticles) : this structure is highly sensible to the type of dispersing agent. An adequate analytical model allowed us to describe more quantitatively this agent effect. The best fits of the aggregate form factor P_{Agg} are shown in plain black curves on Fig.1 : primary aggregate morphology is independent on silica fraction, but it is smaller and denser with TESPT (Fig.1b)) than with OCTEO (Fig.1a)).
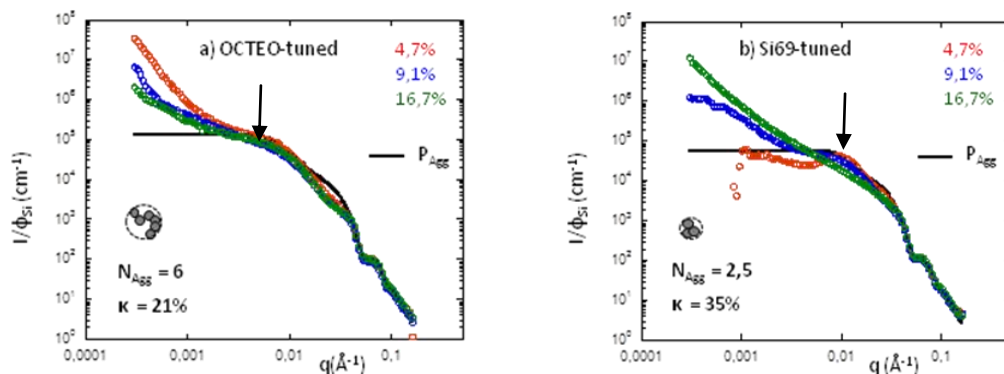

Fig. 1 : Ludox silica dispersion in SBR matrix with increasing silica fraction a) tuned by OCTEO ; b) tuned by Si69

Moreover, the greater increase in scattering at lowest q with Si69 shows that that the primary aggregates organize in a denser network than with OCTEO.

At stretched state, we can observe two main tendencies with increasing strain rate L, illustrated on the example of Fig.2.
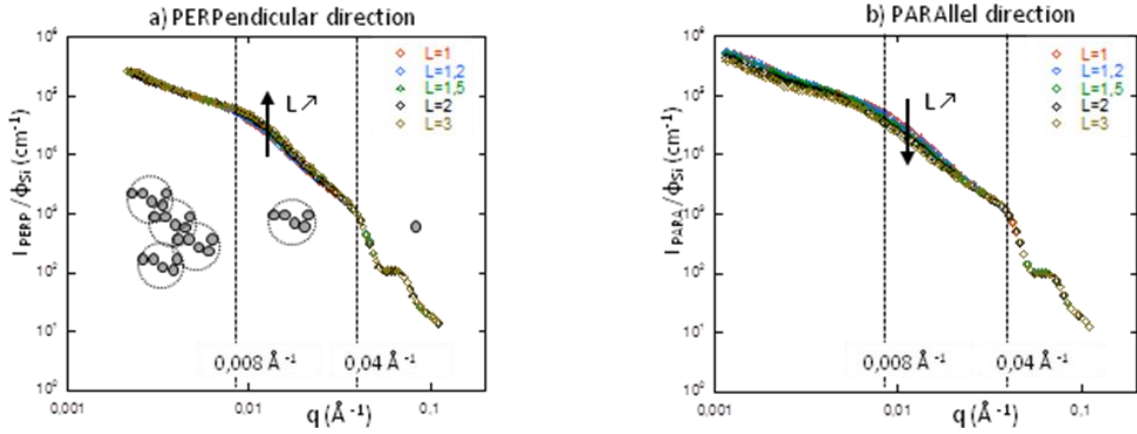
Fig.2 : Evolution of dispersion with increasing strain rate L ;
a) in the PERPendicular direction tuned by OCTEO ; b) in the PARAllel direction tuned by OCTEO

Below $0,008 \text{Å}^{-1}$, we observe in general the deformation of spatial correlations between primary aggregates. In the PARAllel direction (Fig. 2b)), the decrease in scattering shows the decrease in the compactness of the primary aggregate network. By comparison, in the PERP direction (Fig. 2a)), we observe only very slight compaction of the primary aggregate network. In the $[0,008 ; 0,04] \text{Å}^{-1}$ range corresponding to the primary aggregate form factor, changes in scattering with L show that the primary aggregate is modified under traction. However, following quantitatively the evolution in the aggregate form factor with our previous analytical model applied on each pair of spectra is a challenge.

Model nanocomposites made from casting of colloidal silica (Ludox TM40 Aldrich) and polyethylmethacrylate (PEMA) nanolattices were also studied. In this experiment the effects of the filler content and the molecular weight of PEMA (20kg/mol, 50kg/mol and 160kg/mol) were investigated. SAXS spectra normalised by the filler volume fraction are displayed in figure 2.
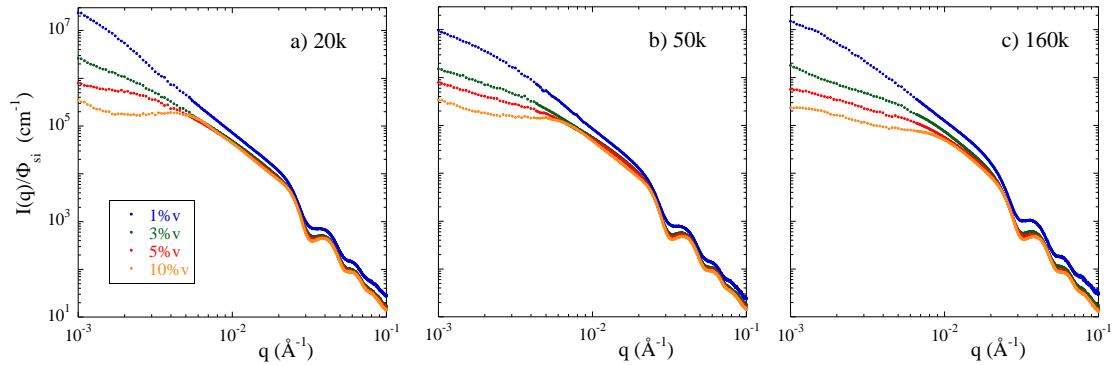

Figure 2: Reduced SAXS scattered intensity I(q)/Φ_{Si} as a function of scattering vector q of PEMA20 (a), PEMA50 (b) and PEMA160 (c) nanocomposites.

These curves display several striking features. First, the high-q data superimpose nicely as expected for identical silica NPs in all samples. Secondly, a common power law is observed at intermediate q, i.e. below ca. $2.3 \ 10^{-2} \ \text{Å}^{-1}$. The exponent lies between -2.3 and -2.4, and it is identical for all three polymer masses. This power-law indicates a common organization of aggregates, with a typical fractal dimension of 2.4. What differs, however, is the extent of the fractal domain. At low chain masses, for 20 and 50 kg/mol, it ranges down to ca. $6 \ 10^{-3} \ \text{Å}^{-1}$, i.e. covers approximately a factor of four in q-range. At the highest mass of 160 kg/mol, the power law is much shorter, covering only a factor of 2 in q-range. The shorter power-law regime suggests that aggregates are smaller, and organize differently on larger scales.

Finally, during this experiment, some tests were also performed on visco-elastic gluten proteins gels to get information about their structure. Data were successfully fitted with models of semi-dilute polymers combined with a fractal structure at larger length scale.